

Enhanced nonlinear frequency conversion and Purcell enhancement at exceptional points

Adi Pick^{1,*}, Zin Lin^{2,*}, Weiliang Jin³, and Alejandro W. Rodriguez³

¹*Department of Physics, Harvard University, Cambridge, MA 02138*

²*John A. Paulson School of Engineering and Applied Sciences,
Harvard University, Cambridge, MA 02138 and*

³*Department of Electrical Engineering,
Princeton University, Princeton, NJ, 08544*

(Dated: January 26, 2020)

Abstract

We derive analytical formulas quantifying radiative emission from subwavelength emitters embedded in triply resonant nonlinear $\chi^{(2)}$ cavities supporting exceptional points (EP) made of dark and leaky modes. We show that the up-converted radiation rate in such a system can be greatly enhanced—by up to two orders of magnitude—compared to typical Purcell factors achievable in non-degenerate cavities, for both monochromatic and broadband emitters. We provide a proof-of-concept demonstration by studying an inverse-designed 2D photonic-crystal slab that supports an EP formed out of a Dirac cone at the emission frequency and a phase-matched, leaky-mode resonance at the second harmonic frequency.

PACS numbers: Valid PACS appear here

* These authors contributed equally to this work.

The increase in radiative emission experienced by a subwavelength particle near a resonant cavity is often characterized by the well-known Purcell factor [1]. In recent work, we presented a generalization of Purcell enhancement that applies to situations involving exceptional points (EP) [2, 3]—spectral singularities in non-Hermitian systems where two or more eigenvectors and their corresponding complex eigenvalues coalesce, leading to a non-diagonalizable, defective Hamiltonian. EPs are attended by a slew of intriguing physical effects [4, 5] and have been studied in various contexts, including lasers, atomic and molecular systems [6, 7], photonic crystals [3, 8, 9], parity-time symmetric lattices [10–22], and optomechanical resonators [23–25]. An important but little explored property of EPs related to light-matter interactions is their ability to modify and enhance a related quantity, the local density of states (LDOS) [2, 3].

In this Letter, we demonstrate that radiative emission at ω_e from a subwavelength particle, e.g. spontaneous emission or fluorescence from atoms or radiation from plasmonic antennas, embedded in a triply resonant nonlinear $\chi^{(2)}$ cavity can be greatly modified and efficiently up-converted to $2\omega_e$ in the vicinity of an EP. The efficiency of such a frequency-conversion process depends strongly on the lifetimes and degree of confinement of the cavity modes [26], which we characterize by deriving a closed-form, analytical formula for the nonlinear Purcell factor: the LDOS or emission rate at $2\omega_e$ from a dipole current source oscillating at ω_e . In particular, we obtain emission bounds applicable to situations involving both monochromatic and broadband emitters, showing that the nonlinear Purcell factor in a cavity supporting an EP at ω_e formed out of dark and leaky modes can generally be more two orders of magnitude larger than that of a non-degenerate cavity, depending on the position of the emitter and on complicated but designable modal selection rules. When combined with recently demonstrated inverse-designed structures optimized to enhance nonlinear interactions [3, 27], the proposed EP enhancements could lead to several orders-of-magnitude larger luminescence efficiencies.

The key to enhancing the LDOS at an EP is to exploit the intricate physics arising from the coalescence of dark and leaky (lossy) resonances. Featuring infinite lifetimes and vanishing decay rates, dark modes are by definition generally inaccessible to external coupling. Consequently, an emitter on resonance with a dark mode cannot radiate unless it is also coupled to a leaky mode. Such a shared resonance underlies the monochromatic LDOS enhancements at EPs described recently in Refs. [2, 3], which showed that the LDOS at an EP exhibits a narrowed, squared Lorentzian lineshape whose peak is four times larger than the maximum LDOS at a non-degenerate resonance. More generally, for an EP of order n , the maximum enhancement factor scales as

$\sqrt{n^3}$ [3]. Although such an effect makes it possible to enhance monochromatic emission near the EP resonance, the existence of a sum rule [28], which forces the frequency-integrated LDOS over the resonance bandwidth to be a constant, prohibits any enhancement in the case of broadband emitters (e.g. fluorescent molecules). In this work, we exploit a coupled-mode theory framework to show that in contrast to the linear LDOS, both the monochromatic and frequency-integrated radiation rate of a dipolar emitter in a nonlinear medium can be enhanced in the presence of an EP. We buttress our theoretical predictions with a concrete physical example: a 2D PhC slab designed to support an EP at ω_e and a leaky (phase-matched) resonance at $2\omega_e$. Furthermore, we consider individual emitters as well as uniform distributions of incoherent emitters throughout the crystal, showing that EPs can enhance emission in both cases.

Coupled-mode analysis.— To understand the impact of EPs on nonlinear frequency conversion, we consider a generic system involving a degenerate (a_1, b_1) tuple of dark and leaky modes at ω_1 and a single mode a_2 at ω_2 . Such a system, shown schematically in Fig. 1, is well described by the following coupled-mode equations (CME) [29]:

$$\frac{da_1}{dt} = i\omega_1 a_1 + i\kappa b_1 - i\omega_1 (\beta_1 a_2 a_1^* + \beta_3 a_2 b_1^*) + s(t) \quad (1)$$

$$\frac{db_1}{dt} = i\omega_1 b_1 - \gamma_1 b_1 + i\kappa a_1 - i\omega_1 (\beta_2 a_2 b_1^* + \beta_3 a_2 a_1^*) \quad (2)$$

$$\frac{da_2}{dt} = i\omega_2 a_2 - \gamma_2 a_2 - i\omega_1 (\beta_1 a_1^2 + \beta_2 b_1^2 + \beta_3 a_1 b_1) \quad (3)$$

Mode a_1 is dark while b_1 and a_2 have decay rates γ_1 and γ_2 , respectively. The two degenerate modes are coupled to one another via the linear coefficient κ and nonlinearly coupled to a_2 by a parametric $\chi^{(2)}$ nonlinear process characterized by mode-overlap factors β_s [26, 29], defined further below in terms of the linear cavity fields. Solving the CMEs in the absence of nonlinearities, one finds that for $\kappa \geq \gamma_1/2$, the frequencies and decay rates of the coupled modes are given by $\omega_{\pm} = \omega_1 \pm \sqrt{\kappa^2 - \gamma_1^2/4}$ and $\gamma_1/2$, respectively, where the latter is independent of κ . In particular, the two degenerate modes coalesce at $\kappa_{\text{EP}} = \gamma_1/2$, forming an EP at the complex frequency $\omega_1 - i\gamma_1/2$. In the limit $\kappa \rightarrow \infty$ of far-apart mode frequencies, one recovers the well-known, non-degenerate (ND), single-mode description of second-harmonic generation [29], which we compare against when considering any enhancements arising from the EP [30]. Note that in these CMEs, the term $s(t)$ represents a dipole current source positioned in such a way so as to exclusively couple to the dark mode, a situation that is illustrated with a concrete physical example further below. Since such a term is meant to model a weak emitter (except in the case of gain

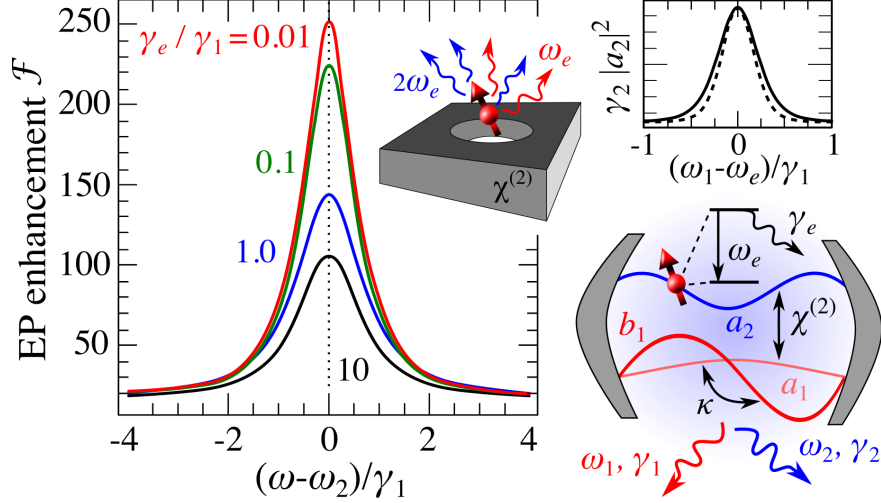


FIG. 1. Schematic of a dipole emitter (ω_e, γ_e) embedded in a triply resonant $\chi^{(2)}$ nonlinear cavity supporting an exceptional point (EP). The cavity consists of two degenerate resonances (a_1, b_1) at ω_1 that are coupled to one another via a linear coupling rate κ and nonlinearly coupled to a harmonic mode of frequency $\omega_2 = 2\omega_1$ and decay rate γ_2 by the $\chi^{(2)}$ process. An EP is formed out of the dark mode a_1 and the leaky mode b_1 of decay rate γ_1 when $\kappa = \gamma_1/2$. The EP leads to enhanced emission at the harmonic frequency, captured in the main plot (left) by the EP enhancement factor $\mathcal{F} = \frac{\gamma_1 |a_2^{\text{EP}}|^2}{\gamma_1 |a_2^{\text{ND}}|^2}$, the ratio of the emission rate around ω_2 at the EP to that of a non-degenerate (ND) system with a single mode at ω_1 of the same effective decay rate $\gamma_1/2$. Here, \mathcal{F} is plotted with respect to the frequency detuning $(\omega - \omega_2)/\gamma_1$ and for multiple $\frac{\gamma_e}{\gamma_1}$. The upper-right inset shows the second-harmonic emission rate $\gamma_2 |a_2|^2$ as a function of detuning $\frac{(\omega_e - \omega_1)}{\gamma_1}$ in the limit of a monochromatic emitter, $\gamma_e \rightarrow 0$, for both EP (solid) and ND (dashed) systems. For convenience, both emission rates have been normalized to have the same peak amplitude.

media), we primarily focus on the so-called small-signal or non-depletion regime where one can neglect the nonlinear terms responsible for down-conversion (e.g. $\beta_1 a_2 a_1^*$).

Before delving further into the nonlinear equations, it is instructive to briefly review the mechanism of LDOS enhancement in the linear regime of $\beta = 0$. Consider a monochromatic source $s(t) = s_0 e^{i\omega_e t}$ that is on-resonance with the cavity, i.e. $\omega_e = \omega_1$. Solving the CMEs, one finds that the steady-state mode amplitudes at the EP are $a_1^{\text{EP}} = 4s_0/\gamma_1$ and $b_1^{\text{EP}} = 2is_0/\gamma_1$, whereas in the ND limit of $\kappa \rightarrow \infty$, $a_1^{\text{ND}} = b_1^{\text{ND}} = s_0/\gamma_1$. Since the LDOS or radiated power is given by $\gamma_1 |b_1|^2$, it follows that the EP produces an enhancement factor $\frac{\gamma_1 |b_1^{\text{EP}}|^2}{\gamma_1 |b_1^{\text{ND}}|^2} = 4$, a result recently derived in Ref. [2] by a perturbative expansion of the Green's function based on Jordan eigenvectors but which also follows from the coupled-mode picture above (see supplemental materials). We

emphasize that such an enhancement can be realized despite the fact that both the EP and ND resonances exhibit the same effective decay rate $\gamma_1/2$, indicating that the enhancement does not arise from an otherwise trivial increase in resonant lifetimes but rather from a constructive interference of the two modes, which leads to both narrowing and amplification of the cavity spectrum [2]. Unfortunately, such an enhancement disappears when considering the frequency-integrated emission from a broadband source, a consequence of a general sum rule (derived from causality [28]) which implies that $\int \gamma_1 |b_1^{\text{EP}}(\omega)|^2 d\omega = \int \gamma_1 |b_1^{\text{ND}}(\omega)|^2 d\omega$. As we show below, however, such a sum rule no longer seems to be valid in the case of finite $\beta \neq 0$.

Consider a typical Lorentzian source, $s(t) = \int_{-\infty}^{\infty} \frac{\sqrt{\gamma_e}}{\gamma_e + i(\omega - \omega_e)} e^{i\omega t} d\omega$, of frequency ω_e and decay rate γ_e , and whose Fourier amplitude $s(\omega)$ is normalized so that $\int |s(\omega)|^2 d\omega = \pi$. Solving the CMEs in the non-depletion regime yields the amplitude a_2 of the harmonic mode as a convolution,

$$a_2(\omega) = \frac{i\omega_1/2}{i(\omega - \omega_2) + \gamma_2} \int_{-\infty}^{\infty} dq \left[\beta_1 a_1(\omega) a_1(\omega - q) + \beta_2 b_1(\omega) b_1(\omega - q) + \beta_3 a_1(\omega) b_1(\omega - q) \right], \quad (4)$$

in terms of the mode amplitudes,

$$a_1(\omega) = \frac{s(\omega) \sqrt{\gamma_e} (\gamma_1 + i(\omega - \omega_1))}{(\kappa^2 + (\omega - \omega_1)(i\gamma_1 - \omega + \omega_1)) (\gamma_e + i(\omega - \omega_e))} \quad (5)$$

$$b_1(\omega) = \frac{is(\omega) \sqrt{\gamma_e} \kappa}{(\kappa^2 + (\omega - \omega_1)(i\gamma_1 - \omega + \omega_1)) (\gamma_e + i(\omega - \omega_e))}. \quad (6)$$

which can be evaluated to yield closed-form, analytical solutions (see supplemental materials). In the particular limit of a monochromatic source with $\gamma_e \ll \gamma_1$, the emission rate at the harmonic frequency, $\gamma_2 |a_2(\delta)|^2$, or nonlinear LDOS can be written as:

$$\gamma_2 |a_2^{\text{EP}}(\delta)|_{\gamma_e \rightarrow 0}^2 = \frac{64\pi^2 \zeta |s|^4}{\gamma_1^5 (4\delta^2 + 1)^4 (4\delta^2 + \zeta^2)} \left[16\beta_1^2 (\delta^2 + 1)^2 + 4\beta_3^2 (\delta^2 + 1) + 8\beta_1 (\beta_2 (\delta^2 - 1) - 2\beta_3 (\delta^3 + \delta)) - 4\beta_2 \beta_3 \delta + \beta_2^2 \right], \quad (7)$$

where $\delta = \frac{\omega_1 - \omega_e}{\gamma_1}$ is the normalized frequency detuning of the emitter from the cavity resonance and $\zeta = \gamma_2/\gamma_1$. Evidently, the output spectrum assumes a narrowed and highly non-Lorentzian lineshape, a signature of the EP. In the opposite limit of a broadband source with $\gamma_e \gg \gamma_1$, the relevant quantity to consider is the integrated LDOS near ω_2 , given by:

$$\begin{aligned}
\int \gamma_2 |a_2^{\text{EP}}(\omega)|^2 d\omega \Big|_{\gamma_e \gg \gamma_1} &\approx \frac{\pi^3 |s|^4}{4608 \gamma_1^5 (\zeta + 1)^3} \left(\frac{\gamma_1}{\gamma_e} \right)^2 \left[\beta_1^2 (237312 \zeta^2 + 638208 \zeta + 460800) \right. \\
&- 2\beta_2 \beta_1 (29952 \zeta^2 + 89856 \zeta + 92160) + \beta_2^2 (6912 \zeta^2 + 20736 \zeta + 18432) \\
&\left. + \beta_3^2 (29952 \zeta^2 + 89856 \zeta + 73728) \right], \tag{8}
\end{aligned}$$

To quantify the impact of these spectral modifications, we compare the emission rates at the EP against those obtained in the ND scenario, given by:

$$\gamma_2 |a_2^{\text{ND}}(\delta)|^2 \Big|_{\gamma_e \rightarrow 0} = \frac{4\pi^2 (\beta_1 + \beta_2 + \beta_3)^2 \zeta |s|^4}{\gamma_1^5 (4\delta^2 + 1)^2 (4\delta^2 + \zeta^2)} \tag{9}$$

$$\int \gamma_2 |a_2^{\text{ND}}(\omega)|^2 d\omega \Big|_{\gamma_e \gg \gamma_1} = \frac{\pi^3 (\beta_1 + \beta_2 + \beta_3)^2 |s|^4}{\gamma_1^5 (\zeta + 1)} \left(\frac{\gamma_1}{\gamma_e} \right)^2 \tag{10}$$

Figure 1 shows the nonlinear EP enhancement factor, $\mathcal{F}(\omega, \gamma_e) = \frac{|a_2^{\text{EP}}(\omega, \gamma_e)|^2}{|a_1^{\text{ND}}(\omega, \gamma_e)|^2}$, which is the ratio of the emission rate around ω_2 at the EP to that in the ND scenario for the typical situation of an emitter that is resonantly coupled to the fundamental cavity frequency, i.e. $\omega_e = \omega_1$. In particular, the figure shows \mathcal{F} as a function of the output frequency $(\omega - \omega_2)/\gamma_1$ and for multiple values of γ_e/γ_1 when all of the nonlinear coupling coefficients except the one pertaining to the dark mode vanish, i.e. $\beta_1 \neq 0$, $\beta_2 = \beta_3 = 0$. Such a nonlinear configuration belies one of the main results of this work, which follows from (9) and (10): the largest radiation rates and therefore Purcell enhancements are achieved when the dipole emitter couples exclusively to the dark mode and when only the latter couples strongly to the harmonic mode. Evaluating \mathcal{F} at $\omega = \omega_2$ and taking the limit of $\gamma_e \rightarrow 0$ or equivalently, evaluating the ratio of (7) and (9) in the limit of zero detuning $\delta = 0$, yields a maximum enhancement factor of 256. The (top-right) inset of Fig. 1 shows the dependence of the nonlinear LDOS (7) with respect to the emitter detuning δ in the monochromatic regime $\gamma_e \rightarrow 0$, showing a slightly narrowed EP spectrum compared to the ND scenario (both spectra are normalized to have the same peak amplitude for clarity). Notably, one finds that compared to the linear scenario discussed above, the nonlinear spectrum undergoes significantly less narrowing, evidence that the frequency-integrated emission can also be enhanced. Indeed, focusing in the case of a broadband emitter with $\gamma_e \gg \gamma_1$, e.g. a fluorescent molecule [31], and taking the ratio of (8) and (10), one finds that the frequency-integrated emission can be enhanced by a factor of 100.

The aforementioned LDOS enhancements at the EP can be understood intuitively from a recently derived sum rule [28]. In the linear regime, causality demands that when two non-degenerate resonances of equal bandwidths γ merge to form an EP, the resulting LDOS spectrum becomes a squared Lorentzian [32] and obeys the sum rule [28], $\sum_i \int \frac{s_i^2 \gamma}{\delta^2 + \gamma^2} d\delta = \int \frac{2s_{\text{EP}}^2 \gamma^3}{(\delta^2 + \gamma^2)^2} d\delta$, where $s_{\text{EP}}^2 = s_1^2 + s_2^2$ and $s_{1,2}$ denote the coupling strengths of a dipole source which generally couples to both modes. It follows from the sum rule that at an EP and in the special case of identical coupling strengths, $s_1 = s_2 = s_{\text{ND}}$, the mode volume of the cavity resonance decreases (and hence the coupling rate of an emitter increases) so that $s_{\text{ND}} = s_{\text{EP}}/\sqrt{2}$, but only at the expense of an effectively narrower cavity bandwidth. Such a multi-modal interference phenomenon also leads to an effective increase in the nonlinear coupling coefficient, with $\beta_{\text{ND}} = 0.5\beta_{\text{EP}}$ (see supplemental materials). Both effects combine to increase nonlinear emission by two orders of magnitude.

Proof-of-concept demonstration.— One way to realize an EP of coalescent dark and leaky modes is by exploiting Dirac cones [8], which are linear conical dispersions in the band structure of PhCs formed out of the degeneracy of modes belonging to different symmetry representations. Here, we employ recently developed inverse-design techniques [3] to design a proof-of-concept PhC exhibiting a Dirac cone at $\omega_1 = \omega_e$ and a leaky mode at $2\omega_1$, both realized at the Γ point ($\mathbf{k} = 0$) of the crystal. Figure 2(a) shows a schematic of the PhC unit cell of size $a \times a$, with the Dirac point at ω_1 formed by an accidental degeneracy of monopolar (M1) and a dipolar (D) modes, while the second-harmonic resonance consists of a monopolar, higher-order field (M2). Here, black/white regions denote relative dielectric $\epsilon_r = 5.5$ and vacuum $\epsilon_r = 1$ permittivities, respectively. We introduce non-Hermiticity to the system by adding a small amount of absorption ($\text{Im}[\epsilon_r] \neq 0$) along the nodal line of M1, which renders the other two modes (D and M2) leaky while keeping M1 dark. By analogy, we identify M1 as a_1 , D as b_1 , and M2 as a_2 . Given the mode profiles (insets), we employ perturbation theory [33] to obtain the corresponding decay rates, $\gamma_{\text{D}}/\omega_1 \approx 10^{-4}$ and $\gamma_{\text{M2}} \approx 2\gamma_{\text{D}}$. As described in Ref. [3], the band structure of the PhC in the vicinity of ω_1 can be described by an effective 2×2 Hamiltonian [8], $\begin{pmatrix} \omega_1 & v_g k \\ v_g k & \omega_1 + i\gamma_{\text{D}} \end{pmatrix}$, where k denotes the Bloch wave number and v_g is the group velocity (the slope of the conical dispersion). Such a system exhibits an EP at $k_{\text{EP}} = \gamma_{\text{D}}/2v_g$. Assuming that dielectric regions possess a non-zero second-order susceptibility $\chi^{(2)}$, the nonlinear overlap factors are given by:

$$\beta = \frac{\int \chi^{(2)} E_{\text{M2}}^* E_i E_j d\mathbf{r}}{\sqrt{\int \epsilon_r |E_{\text{M2}}|^2 d\mathbf{r}} \sqrt{\int \epsilon_r |E_i|^2 d\mathbf{r}} \sqrt{\int \epsilon_r |E_j|^2 d\mathbf{r}}},$$

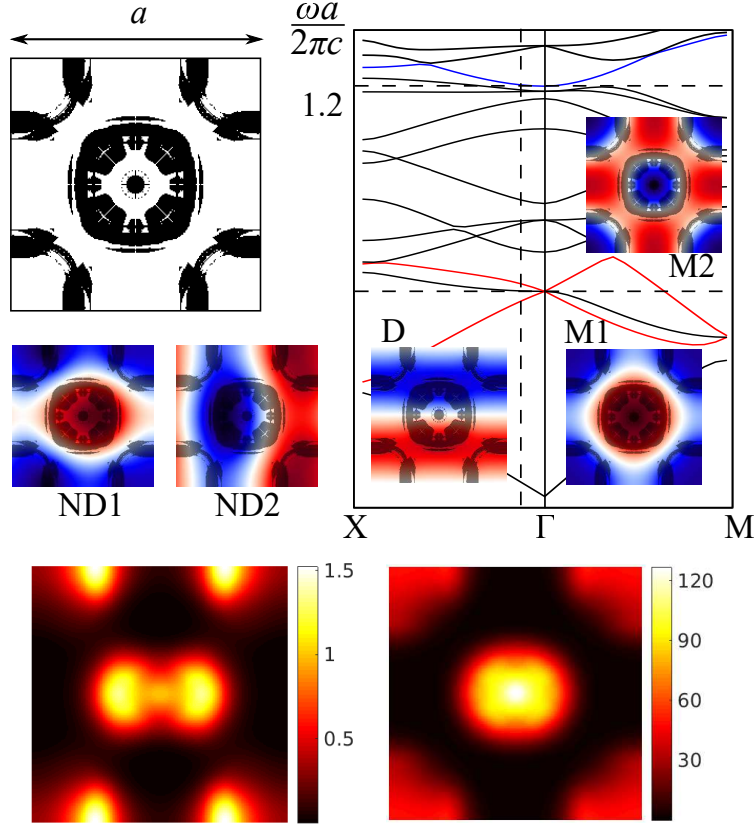


FIG. 2. Inverse-designed 2D square PhC (unit cell). Dark/white regions represent relative permittivities $\epsilon_r = 5.5/1$. The corresponding band structure exhibits a Dirac cone (red bands) centered at ω_1 and a leaky second-harmonic resonance (blue band) around $\omega_2 = 2\omega_1$. A Dirac degeneracy at Γ is formed by monopolar (M1) and dipolar (D) modes while the second-harmonic resonance is a higher-order monopolar mode (M2). Non-hermiticity is introduced by inserting a small amount of dielectric loss along the nodal line of the M1 mode, allowing realization of an EP near ω_1 . Nondegenerate modes (ND1, ND2) at $k_x a/2\pi \approx 0.1$ (vertical dashed line in the band diagram) are also depicted, illustrating mode mixing between the monopole and dipole modes. The lower panels show the spatially varying nonlinear LDOS $\int \gamma_2 |a_2|^2 dx$, i.e. the emission rate at $2\omega_e$ from monochromatic dipole sources oscillating at $\omega_e = \omega_1$, in both ND (left) and EP (right) scenarios, illustrating a maximum enhancement factor of ≈ 127 at the center of the unit cell.

with $i, j \in \{M1, D\}$ and $E_{\{M1, M2, D\}}$ denoting the electric fields of the M1, M2 and D modes.

Our choice of mode symmetries guarantees nearly optimal nonlinear coupling coefficients for enhancing \mathcal{F} . In particular, we find that in this structure, $\beta_1 \approx 0.07(\chi^{(2)}/\sqrt{\lambda_1^2})$, $\beta_2/\beta_1 \approx 0.04$, and $\beta_3/\beta_1 \approx 0$. Moreover, by construction a dipole emitter located at the center of the unit cell couples solely to the dark mode (M1). In the coupled-mode theory framework, the strength of

the internal dipole current coupling to M1 is given by $s(\mathbf{r}_0, t) = s(t)E_{M1}(\mathbf{r}_0)/2 \int \epsilon_r |E_{M1}|^2 d\mathbf{r}$, where \mathbf{r}_0 is at the center of the unit cell. Note that technically, what one computes at k_{EP} is the LDOS-per-k or so-called mutual DOS [34], corresponding to emission from an array of coherent, dipole emitters periodically placed at the center of each unit cell. Hence, angular emission is channeled into the EP modes at k_{EP} and up-converted into the corresponding phase-matched second harmonic mode at $2k_{EP}$. For sufficiently small $\gamma_D \propto k_{EP} \approx 0$, the phase-matching condition ($k_2 \approx 2k_{EP}$) can be enforced via perturbative fine-tuning of the dielectric structure with the aid of well-known experimental techniques, e.g. thermal, mechanical, or electro-optic post-fabrication mechanisms [35, 36]. Note that our system represents a proof of concept, but that it is straightforward (though computationally intensive) to consider extensions to 3D slab geometries, in which case the non-Hermiticity could stem from radiative rather than dielectric losses.

Figure 2 also shows the mode profile of two ND modes at $k_x a/2\pi \approx 0.1$ (vertical dashed line in the band diagram) which merge to form the EP in the limit as $k_x \rightarrow k_{EP}$. Note that in this example, the two modes (denoted as ND1 and ND2) exhibit equal decay rates but slightly different coupling strengths, $s_{ND1} \approx 0.76s_{EP}$ and $s_{ND2} \approx 0.64s_{EP}$, and nonlinear coefficients, $\beta_{ND1} \approx 0.62\beta_{EP}$ and $\beta_{ND2} \approx 0.41\beta_{EP}$. Comparing against ND1, i.e. the more localized of the two ND resonances, we find that the EP leads to monochromatic and frequency-integrated enhancement factors of 127 and 32, respectively. Another important quantity characterizing SE from PhCs is the spectral density of states [34] (SDOS), obtained by integrating the LDOS-per-k over the entire unit cell. The SDOS quantifies large-area emission from an incoherent ensemble of dipole emitters uniformly distributed throughout the PhC, and is relevant to wide-area fluorescence and lasing [31]. In the above formulation, the nonlinear SDOS is given by $\int \gamma_2 |a_2(\mathbf{r}, \omega)|^2 d\mathbf{r}$, where the spatial dependence in the mode amplitude a_2 comes from the variation of the dipole coupling in space. More precisely, the coupling of a source at \mathbf{r} to the fundamental modes is represented by two separate source terms, $s_a(\mathbf{r}) = \frac{E_{M1}(\mathbf{r})}{2 \int \epsilon_r E_{M1}(\mathbf{r}) d\mathbf{r}}$ and $s_b(\mathbf{r}) = \frac{E_D(\mathbf{r})}{2 \int \epsilon_r E_D(\mathbf{r}) d\mathbf{r}}$, in the equations for a_1 and b_1 , respectively (see supplemental materials). In contrast, (21)–(23) capture only the optimal situation in which $\mathbf{r} = \mathbf{r}_0$ and hence $s_b(\mathbf{r}_0) = 0$. Given the concrete design above, one can compute the spatially varying coupling coefficients for both the EP and ND scenarios, which are plotted in the lower panel of Fig. 2. For broadband emitters with linewidths $\gamma_e \gg \gamma_1$, the quantity of interest is the frequency-integrated SDOS, in which case the enhancement ratio, $\frac{\int \int |a_2^{EP}|^2 d\omega d\mathbf{r}}{\int \int |a_2^{ND}|^2 d\omega d\mathbf{r}}$, which compares second-harmonic emission rates into the selective angular channel specified by \mathbf{k} (near-normal incidence), is 15.

Concluding remarks.— To summarize, we have shown that the efficiency of nonlinear frequency conversion processes can be greatly enhanced in cavities featuring EPs. Our derived bounds on the possible nonlinear Purcell factors achievable in EP systems show that the degree of enhancement depends on complicated but tunable modal selection rules and are optimal when the emission sources couple primarily to dark modes. In combination with recently demonstrated inverse-designed structures optimized to enhance nonlinear overlaps [27], the proposed EP enhancements could lead to orders-of-magnitude larger nonlinear interactions and emission efficiencies. While luminescence enhancements at EPs in linear media are nullified in the case of broadband emitters, nonlinear Purcell factors can be enhanced by two orders of magnitudes even when the emission bandwidth is much larger than the cavity bandwidth. Although we illustrated these ideas by examining a simple proof-of-concept 2d PhC design, these predictions could also be tested in a wide variety of structures, including highly nonlinear mid-infrared quantum wells [37] or microwave super-conducting qubit [38] platforms. Finally, we expect that similar or even potentially larger enhancements can arise in systems supporting higher-order exceptional points [3] or other nonlinear processes, e.g. third-harmonic generation, four-wave mixing, and two-photon down-conversion, with potential applications to quantum information science.

I. SUPPLEMENT

We provide a more detailed analysis of the coupled-mode equations in the main text, which describe two optical resonances (a dark and leaky mode) linearly coupled to one another to form an exceptional point (EP), and nonlinearly coupled to a second-harmonic mode via a Pockels $\chi^{(2)}$ medium. We show that relative to non-degenerate scenarios, radiative emission at the up-converted frequency from a source which couples only to the dark mode is enhanced due to an effective reduction in the mode volume of the cavity at the emission wavelength, which manifests as an increase in the local density of states and nonlinear overlap coefficients governing second-harmonic generation. Finally, we provide a full formula for the up-converted (second-harmonic) emission rate of a dipole oscillating at the EP frequency.

A. Spectral narrowing and mode reduction at an exceptional point

In Ref. [2], we showed via direct manipulation of Maxwell's equations that an optical cavity supporting an EP will exhibit an amplified but narrowed (squared Lorentzian) spectrum. We also exploited a well-known sum-rule which states that the frequency-integrated density of states must be conserved [28] in order to argue that the modified LDOS lineshape necessarily sets an upper bound of four on the peak enhancement. Below, we show that both the spectral enhancement and sum rule also follow from the CMEs above.

Consider the linearized, coupled-mode equations ($\beta = 0$):

$$\frac{da_1}{dt} = i\omega_1 a_1 + i\kappa b_1 + s(t) \quad (11)$$

$$\frac{db_1}{dt} = (i\omega_1 - \gamma_1)b_1 + i\kappa a_1. \quad (12)$$

The LDOS spectrum of the system is given by:

$$\gamma_1 |b_1(\omega)|^2 = \frac{\gamma_1 \kappa^2 |s(\omega)|^2}{[\kappa^2 - (\omega - \omega_1)^2]^2 + \gamma_1^2 (\omega - \omega_1)^2} \quad (13)$$

It follows that at the EP, $\kappa = \gamma_1/2$, the spectrum becomes a pure, squared Lorentzian,

$$\gamma_1 |b_1^{\text{EP}}(\omega)|^2 = \frac{2|s(\omega)|^2 \left(\frac{\gamma_1}{2}\right)^3}{\left[\left(\frac{\gamma_1}{2}\right)^2 + (\omega - \omega_1)\right]^2}, \quad (14)$$

centered around ω_1 and with bandwidth $\gamma_1/2$. Taking the strong-coupling limit $\kappa \gg \gamma_1$ of two coupled but highly non-degenerate (ND) resonances, one finds:

$$\gamma_1 |b_1^{\text{ND}}(\omega)|^2 = \frac{\frac{\gamma_1}{4}|s(\omega)|^2}{\left(\frac{\gamma_1}{2}\right)^2 + [\omega - (\omega_1 + \kappa)]^2} + \frac{\frac{\gamma_1}{4}|s(\omega)|^2}{\left(\frac{\gamma_1}{2}\right)^2 + [\omega - (\omega_1 - \kappa)]^2} - \frac{\gamma_1 |s(\omega)|^2}{2\kappa^2} + \mathcal{O}\left[\frac{\gamma_1}{\kappa}\right]^3 \quad (15)$$

Hence, in the $\kappa \rightarrow \infty$ limit, the spectrum becomes a sum of identical Lorentzians centered around the eigenfrequencies $\omega_1 \pm \kappa$ and with bandwidths $\gamma_1/2$. Notably, their individual peak amplitudes are exactly four times smaller than that of the squared Lorentzian:

$$\frac{\gamma_1 |b_1^{\text{EP}}(\omega = \omega_1)|^2}{\gamma_1 |b_1^{\text{ND}}(\omega = \omega_1 \pm \kappa)|^2} = 4. \quad (16)$$

Essentially, one could argue that at an EP, the mode volume of the cavity resonance experiences an effective reduction of $\sqrt{2}$ but only at the expense of a narrower bandwidth. In particular, integrating (14) and (15), one finds that

$$\int \gamma_1 |b_1^{\text{EP}}(\omega)|^2 d\omega = \int \gamma_1 |b_1^{\text{ND}}(\omega)|^2 d\omega, \quad (17)$$

in agreement with the aforementioned sum rule [28].

B. Nonlinear-overlap enhancement

In the main text, we showed and argued that the effectively smaller mode volume associated with an EP also leads to a two-fold increase in the nonlinear overlap coefficients. Here, we show explicitly how such an increase manifests in the CMEs.

The Hamiltonian corresponding to the linear, coupled-mode system above is given by:

$$\mathcal{H} = \begin{pmatrix} \omega_1 & \kappa \\ \kappa & \omega_1 - i\gamma_1 \end{pmatrix}. \quad (18)$$

For $\kappa \neq \gamma_1/2$, \mathcal{H} can be diagonalized such that the mode amplitudes $\vec{a}_1 = (a_1, b_1)$ can be transformed into the diagonal basis $\vec{a}'_1 = (a'_1, b'_1)$ by a linear, unitary transformation matrix S , such that $\vec{a}_1 = S\vec{a}'_1$. In the strong-coupling limit $\kappa \rightarrow \infty$ of ND resonances, the transformation matrix is $S = \begin{pmatrix} -\frac{1}{\sqrt{2}} & \frac{1}{\sqrt{2}} \\ \frac{1}{\sqrt{2}} & \frac{1}{\sqrt{2}} \end{pmatrix}$. Writing the amplitude of the second-harmonic mode in the non-depletion limit,

$$a_2(\omega) = \frac{-i\omega_1 (\beta_1 a_1^2 + \beta_2 b_1^2 + \beta_3 a_1 b_1)}{\gamma_2 + i(\omega - \omega_2)},$$

in terms of the ND resonance (i.e. taking $\vec{a}_1 \rightarrow S\vec{a}'_1$), one finds that the amplitude in the ND limit $\kappa \rightarrow \infty$ is given by:

$$a_2(\omega) = \frac{-i\omega_1}{\gamma_2 + i(\omega - \omega_2)} \frac{(\beta_1 + \beta_2 + \beta_3)}{2} (a'_1)^2. \quad (19)$$

Thus, the nonlinear overlap coefficient of the ND system is related to the corresponding overlap factors of the system at the EP by the relation:

$$\beta^{\text{ND}} = \frac{(\beta_1 + \beta_2 + \beta_3)}{2}. \quad (20)$$

C. Nonlinear EP enhancement formula

The nonlinear CMEs describing emission from a dipolar source embedded in the triply resonant cavity above are (in the non-depletion regime):

$$\frac{da_1}{dt} = i\omega_1 a_1 + i\kappa b_1 + s_a(t) \quad (21)$$

$$\frac{db_1}{dt} = (i\omega_1 - \gamma_1)b_1 + i\kappa a_1 + s_b(t) \quad (22)$$

$$\frac{da_2}{dt} = i\omega_2 a_2 - \gamma_2 a_2 - i\omega_1 (\beta_1 a_1^2 + \beta_2 b_1^2 + \beta_3 a_1 b_1) \quad (23)$$

Here, we assume that the two cavity resonances are frequency-matched for second-harmonic generation, so that $\omega_2 = 2\omega_1$. Assuming a Lorentzian dipole source located at some position \vec{r} , the coupling amplitudes in (21) and (22) are $s_{a/b}(t) = \left(\frac{E_{a/b}(\vec{r})}{2 \int \epsilon_r |\vec{E}_{a/b}|^2 d\vec{r}} \right) \int_{-\infty}^{\infty} \frac{\sqrt{\gamma_e}}{\gamma_e + i(\omega - \omega_e)} e^{i\omega t} d\omega$. To obtain an explicit expression for $a_2(\omega)$, it suffices to Fourier transform (23), in which case one finds that the amplitude at the second harmonic depends on a convolution of the linear modes at ω_1 . Focusing on the EP scenario ($\kappa = \gamma_1/2$) and defining $\delta = \omega - 2\omega_1$, one obtains:

$$\begin{aligned} a_2^{\text{EP}}(\omega) = & -8\pi\gamma_e \left\{ i\beta_3 \left[2s_a s_b (\gamma_1^2 \delta + i\gamma_1^3 + \gamma_1 \delta (4\gamma_e + i(-4\omega_e + 5\omega - 6\omega_1))) + 2\delta^2 (i\gamma_e + \omega_e - \omega + \omega_1) \right] \right. \\ & + \gamma_1 s_a^2 (2\gamma_1 + i\delta) (2\gamma_1 + 2\gamma_e + i(-2\omega_e + 3\omega - 4\omega_1)) + \gamma_1 \delta s_b^2 (2i\gamma_1 + 2i\gamma_e + 2\omega_e - 3\omega + 4\omega_1) \left. \right] \\ & + \beta_1 \left[2\gamma_1 s_a s_b (2\gamma_1 + i\delta) (2i\gamma_1 + 2i\gamma_e + 2\omega_e - 3\omega + 4\omega_1) \right. \\ & + s_a^2 (8\gamma_1^3 + \gamma_1^2 (10\gamma_e + i(-10\omega_e + 21\omega - 32\omega_1)) + 4\gamma_1 \delta (3i\gamma_e + 3\omega_e - 4\omega + 5\omega_1) \\ & \left. - 4\delta^2 (\gamma_e + i(-\omega_e + \omega - \omega_1))) + \gamma_1^2 s_b^2 (-2\gamma_1 - 2\gamma_e + 2i\omega_e - 3i\omega + 4i\omega_1) \right] \\ & \left. - \beta_2 \left[2\gamma_1 \delta s_a s_b (2\gamma_1 + 2\gamma_e + i(-2\omega_e + 3\omega - 4\omega_1)) + \gamma_1^2 s_a^2 (2\gamma_1 + 2\gamma_e + i(-2\omega_e + 3\omega - 4\omega_1)) \right. \right. \\ & \left. \left. + s_b^2 (\gamma_1^2 (-2\gamma_e + 2i\omega_e - i\omega) + 4\gamma_1 \delta (-i\gamma_e - \omega_e + \omega - \omega_1) + 4\delta^2 (\gamma_e + i(-\omega_e + \omega - \omega_1))) \right] \right\} \\ & / \left\{ [\gamma_1 + i(\omega - 2\omega_1)]^3 [-i\gamma_2 + \omega - 2\omega_1] (\gamma_1 + 2(\gamma_e + i(-\omega_e + \omega - \omega_1)))^2 (-2i\gamma_e - 2\omega_e + \omega) \right\} \end{aligned} \quad (24)$$

Given this unruly but general expression, we consider two main limiting cases in the main text, corresponding to either a monochromatic ($\gamma_e \rightarrow 0$) or broadband ($\gamma_e \gg \gamma_1$) emitter, leading to the equations given in the main text. For comparison, we also consider second-harmonic generation in the ND limit, in which case the steady-state amplitude is given by:

$$a_2^{\text{ND}}(\omega) = \frac{16i\pi\gamma_e\beta^{\text{ND}}s^{\text{ND}}}{(-i\gamma_1 + \delta)(-i\gamma_2 + \delta)(\gamma_1 + 2(\gamma_e + i(-\omega_e + \omega - \omega_1)))(-2i\gamma_e - 2\omega_e + \omega)}, \quad (25)$$

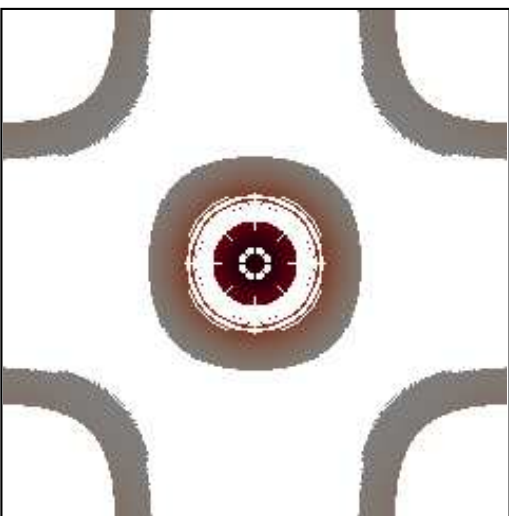
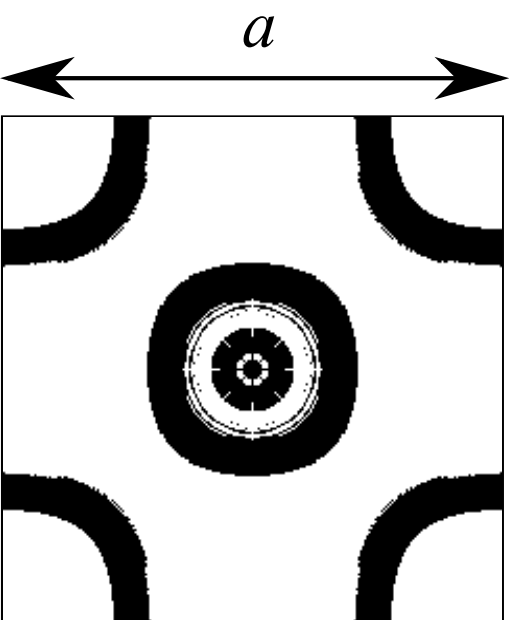
where $s^{\text{ND}} = \frac{s_a + s_b}{\sqrt{2}}$ and $\beta^{\text{ND}} = \frac{\beta_1 + \beta_2 + \beta_3}{2}$.

-
- [1] Edward M Purcell, HC Torrey, and Robert V Pound. Resonance absorption by nuclear magnetic moments in a solid. *Physical review*, 69(1-2):37, 1946.
- [2] A. Pick, B. Zhen, O. D. Miller, C. W. Hsu, F. Hernandez, A. W. Rodriguez, M. Soljačić, and S. G. Johnson. General theory of spontaneous emission near exceptional points. *arXiv*, 1604.06478, 2016.
- [3] Zin Lin, Adi Pick, Marko Lončar, and Alejandro W Rodriguez. Enhanced spontaneous emission at third-order dirac exceptional points in inverse-designed photonic crystals. *Physical Review Letters*, 117(10):107402, 2016.
- [4] Nimrod Moiseyev. *Non-Hermitian Quantum Mechanics*. Cambridge University Press, 2011.
- [5] Tosio Kato. *Perturbation theory for linear operators*. Springer-Verlag Berlin Heidelberg, 1995.
- [6] Michael V. Berry. Physics of nonhermitian degeneracies. *Czechoslovak Journal of Physics*, 54(10), 2004.
- [7] W D Heiss. The physics of exceptional points. *Journal of Physics A: Mathematical and Theoretical*, 45(44):444016, 2012.
- [8] Bo Zhen, Chia Wei Hsu, Yuichi Igarashi, Ling Lu, Ido Kaminer, Adi Pick, Song-Liang Chua, John D. Joannopoulos, and Marin Soljacic. Spawning rings of exceptional points out of dirac cones. *Nature*, 525(7569):354–358, 09 2015.
- [9] Alexander Cerjan, Aaswath Raman, and Shanhui Fan. Exceptional contours and band structure design in parity-time symmetric photonic crystals. *Physical review letters*, 116(20):203902, 2016.
- [10] Carl M. Bender and Stefan Boettcher. Real spectra in non-hermitian hamiltonians having \mathcal{PT} symmetry. *Phys. Rev. Lett.*, 80:5243–5246, 1998.
- [11] Zin Lin, Hamidreza Ramezani, Toni Eichelkraut, Tsampikos Kottos, Hui Cao, and Demetrios N. Christodoulides. Unidirectional invisibility induced by \mathcal{PT} -symmetric periodic structures. *Phys. Rev. Lett.*, 106:213901, 2011.
- [12] Liang Feng, Ye-Long Xu, William S. Fegadolli, Ming-Hui Lu, JoséE. B. Oliveira, Vilson R. Almeida,

- Yan-Feng Chen, and Axel Scherer. Experimental demonstration of a unidirectional reflectionless parity-time metamaterial at optical frequencies. *Nat Mater*, 12(2):108–113, 2013.
- [13] Christian E. Ruter, Konstantinos G. Makris, Ramy El-Ganainy, Demetrios N. Christodoulides, Mordechai Segev, and Detlef Kip. Observation of parity-time symmetry in optics. *Nat Phys*, 6(3):192–195, 2010.
- [14] A. Guo, G. J. Salamo, D. Duchesne, R. Morandotti, M. Volatier-Ravat, V. Aimez, G. A. Siviloglou, and D. N. Christodoulides. Observation of \mathcal{PT} -symmetry breaking in complex optical potentials. *Phys. Rev. Lett.*, 103:093902, 2009.
- [15] Mei C. Zheng, Demetrios N. Christodoulides, Ragnar Fleischmann, and Tsampikos Kottos. \mathcal{PT} optical lattices and universality in beam dynamics. *Phys. Rev. A*, 82:010103, 2010.
- [16] Hamidreza Ramezani, Tsampikos Kottos, Vassilios Kovanis, and Demetrios N. Christodoulides. Exceptional-point dynamics in photonic honeycomb lattices with \mathcal{PT} symmetry. *Phys. Rev. A*, 85:013818, 2012.
- [17] Stefano Longhi and Giuseppe Della Valle. Optical lattices with exceptional points in the continuum. *Phys. Rev. A*, 89:052132, 2014.
- [18] Li Ge and A. Douglas Stone. Parity-time symmetry breaking beyond one dimension: The role of degeneracy. *Phys. Rev. X*, 4:031011, 2014.
- [19] M. Liertzer, Li Ge, A. Cerjan, A. D. Stone, H. E. Türeci, and S. Rotter. Pump-induced exceptional points in lasers. *Phys. Rev. Lett.*, 108:173901, 2012.
- [20] Hossein Hodaei, Mohammad-Ali Miri, Matthias Heinrich, Demetrios N. Christodoulides, and Mercedeh Khajavikhan. Parity-time-symmetric microring lasers. *Science*, 346(6212):975–978, 2014.
- [21] Liang Feng, Zi Jing Wong, Ren-Min Ma, Yuan Wang, and Xiang Zhang. Single-mode laser by parity-time symmetry breaking. *Science*, 346(6212):972–975, 2014.
- [22] B Peng, ŞK Özdemir, S Rotter, H Yilmaz, M Liertzer, F Monifi, CM Bender, F Nori, and L Yang. Loss-induced suppression and revival of lasing. *Science*, 346(6207):328–332, 2014.
- [23] T. Gao, E. Estrecho, K. Y. Bliokh, T. C. H. Liew, M. D. Fraser, S. Brodbeck, M. Kamp, C. Schneider, S. Hofling, Y. Yamamoto, F. Nori, Y. S. Kivshar, A. G. Truscott, R. G. Dall, and E. A. Ostrovskaya. Observation of non-hermitian degeneracies in a chaotic exciton-polariton billiard. *Nature*, 526(7574):554–558, 2015.
- [24] H Xu, D Mason, Luyao Jiang, and JGE Harris. Topological dynamics in an optomechanical system with highly non-degenerate modes. *arXiv preprint arXiv:1703.07374*, 2017.

- [25] H Jing, ŞK Özdemir, H Lü, and Franco Nori. Enhanced optomechanical cooling at high-order exceptional points. *arXiv preprint arXiv:1609.01845*, 2016.
- [26] Robert W. Boyd. *Nonlinear Optics*. Academic Press, California, 1992.
- [27] Zin Lin, Xiangdong Liang, Marko Lončar, Steven G. Johnson, and Alejandro W. Rodriguez. Cavity-enhanced second-harmonic generation via nonlinear-overlap optimization. *Optica*, 3(3):233–238, Mar 2016.
- [28] S. M. Barnett and R. Loudon. Sum rule for modified spontaneous emission rates. *Phys. Rev. Lett.*, 77(12):2444, 1996.
- [29] Alejandro Rodriguez, Marin Soljačić, J. D. Joannopoulos, and Steven G. Johnson. $\chi^{(2)}$ and $\chi^{(3)}$ harmonic generation at a critical power in inhomogeneous doubly resonant cavities. *Optics Express*, 15(12):7303–7318, 2007.
- [30] Note that in principle, coupled-mode theory breaks down in the asymptotic limit of infinite coupling $\kappa \rightarrow \infty$. However, as exemplified in the physical example of Fig. 2 and as follows from the CMEs, similar enhancements are achieved in the more practical and adequate situation of far-separated and well-defined resonances with $\kappa \gg \gamma_1$.
- [31] Bo Zhen, Song-Liang Chua, Jeongwon Lee, Alejandro W Rodriguez, Xiangdong Liang, Steven G Johnson, John D Joannopoulos, Marin Soljačić, and Ofer Shapira. Enabling enhanced emission and low-threshold lasing of organic molecules using special fano resonances of macroscopic photonic crystals. *Proceedings of the National Academy of Sciences*, 110(34):13711–13716, 2013.
- [32] The optical response of a system near a doubly degenerate leaky resonance can be approximated by a second-order, complex pole [ref].
- [33] J. D. Joannopoulos, S. G. Johnson, J. N. Winn, and R. D. Meade. *Photonic crystals: molding the flow of light*. Princeton university press, 2011.
- [34] RC McPhedran, LC Botten, J McOrist, AA Asatryan, C Martijn de Sterke, and NA Nicorovici. Density of states functions for photonic crystals. *Physical Review E*, 69(1):016609, 2004.
- [35] JU Furst, DV Strelakov, Dominique Elser, Mikael Lassen, Ulrik Lund Andersen, Christoph Marquardt, and Gerd Leuchs. Naturally phase-matched second-harmonic generation in a whispering-gallery-mode resonator. *Physical review letters*, 104(15):153901, 2010.
- [36] Xiang Guo, Chang-Ling Zou, Hojoong Jung, and Hong X Tang. On-chip strong coupling and efficient frequency conversion between telecom and visible optical modes. *Physical Review Letters*, 117(12):123902, 2016.

- [37] E Rosencher, A Fiore, B Vinter, V Berger, et al. Quantum engineering of optical nonlinearities. *Science*, 271(5246):168, 1996.
- [38] Gerhard Kirchmair, Brian Vlastakis, Zaki Leghtas, Simon E Nigg, Hanhee Paik, Eran Ginossar, Mazhar Mirrahimi, Luigi Frunzio, Steven M Girvin, and Robert J Schoelkopf. Observation of quantum state collapse and revival due to the single-photon kerr effect. *Nature*, 495(7440):205–209, 2013.



$$\frac{\omega a}{2\pi c}$$

1.2

0.6

